BMC Oral Health

RESEARCH

Open Access

# Effect of pontic volume on fracture resistance of three-unit metal-ceramic fixed dental prostheses: an in vitro and finite element analysis study

Buse Cebi Gul[1*], Erkan Bahce[2], Adem Atmaca[3], Furkan Kuzudisli[4] and Fatih Demirci[5]

## Abstract

**Purpose** This study evaluated the effect of pontic volume on the fracture resistance of three-unit metal-ceramic fixed dental prostheses (FDPs) using in vitro fracture tests and finite element analysis (FEA).

**Materials and methods** Three pontic volume configurations (Small, Medium, and Large) were designed for mandibular posterior three-unit FDPs with second premolar and second molar abutments. Cobalt-chromium (Co-Cr) alloy frameworks were fabricated by direct metal laser sintering. For each configuration, 10 specimens with only metal and 10 specimens with feldspathic porcelain veneers (1.5 mm) were prepared ($N=60$). FEA was performed on metal frameworks under a vertical load of 500 N. Data were analyzed using one-way analysis of variance (ANOVA) and Tukey honestly significant difference (HSD) post-hoc tests($\alpha=0.05$).

**Results** Average fracture loads ranged from $5284.1 \pm 228.85$ N to $6093.5 \pm 330.34$ N in the metal group and from $1506.0 \pm 183.41$ N to $1935.8 \pm 153.06$ N in the porcelain group. All differences between groups were statistically significant ($P<.05$). FEA showed that the maximum von Mises stress at the connector decreased from 740 MPa to 325 MPa as the pontic volume increased. In all groups, fractures occurred predominantly at the connector.

**Conclusions** Increasing the pontic volume significantly improves fracture resistance in both metal and porcelain-veneered restorations. Framework-only FEA showed a reduction in connector stress with increasing pontic volume, which is consistent with the direction of the in vitro findings.

**Keywords** Finite element analysis, Fixed dental prosthesis, Fracture strength, Metal-ceramic, Pontic design

*Correspondence:
Buse Cebi Gul
buse.cebi@hotmail.com
[1]Department of Prosthodontics, Faculty of Dentistry, Inonu University, Eczacılık Cad, Battalgazi/Malatya 44280, Turkey
[2]Department of Mechanical Engineering, Faculty of Engineering, Inonu University, Üniversite Mah., Bilen Sok., 36, Battalgazi/Malatya, Turkey
[3]Department of Mechanical Engineering, Faculty of Engineering, Gaziantep University, 15 Temmuz, Üniversite Blv., Şehitkamil/Gaziantep 27310, Turkey
[4]Department of Mechanical Engineering, Gaziantep University, 15 Temmuz, Üniversite Blv., Şehitkamil/ Gaziantep 27310, Turkey
[5]Özel Beşiroğlu Ağız ve Diş Sağlığı Merkezi, Gebze/Kocaeli, Turkey

© The Author(s) 2026. **Open Access** This article is licensed under a Creative Commons Attribution-NonCommercial-NoDerivatives 4.0 International License, which permits any non-commercial use, sharing, distribution and reproduction in any medium or format, as long as you give appropriate credit to the original author(s) and the source, provide a link to the Creative Commons licence, and indicate if you modified the licensed material. You do not have permission under this licence to share adapted material derived from this article or parts of it. The images or other third party material in this article are included in the article's Creative Commons licence, unless indicated otherwise in a credit line to the material. If material is not included in the article's Creative Commons licence and your intended use is not permitted by statutory regulation or exceeds the permitted use, you will need to obtain permission directly from the copyright holder. To view a copy of this licence, visit http://creativecommons.org/licenses/by-nc-nd/4.0/.

## Introduction

Fixed dental prostheses (FDPs) are prosthetic restorations that replace one or more missing teeth and cannot be removed from the patient's mouth. These prostheses are supported by the natural teeth (abutments) on either side of the missing tooth, supporting an artificial tooth called a pontic [1]. Metal-supported porcelain FDPs are widely used in dentistry due to their high durability, aesthetic appearance, and biocompatibility [2].

The clinical success of FDPs depends on various factors. These include the periodontal status of the abutment teeth, the crown-root ratio, occlusal forces, and prosthesis design [3]. Pontic design directly affects both the durability of the restorative material and the health of the underlying soft tissue [3]. The literature contains several studies examining the factors affecting the fracture strength of FDPs. Finite element analysis (FEA) has been used to evaluate many factors influencing fracture strength in prosthetic dentistry. These studies have assessed the stress distribution and fracture strength of implant and tooth-supported FDPs, particularly by modifying design parameters such as connector design and size, connector height, and veneer-frame thickness ratio [4–7].

In the literature, particularly on the most-studied three-unit restorations, it has been reported that the weakest region is the connector area [8, 9]. Oh and Anusavice [8] demonstrated the decisive effect of connector design on fracture strength. Bataineh et al. [7] showed that increasing the connector size improved fatigue strength. Alberto et al. [6], reported that biomechanical performance improved with increasing connector height. Larsson et al. [10] reported that fracture strength increased significantly with increasing connector diameter. Ogino et al. [11] and Tatarciuc et al. [12] revealed the decisive role of connector size and cross-sectional form on fracture strength. All these studies demonstrate that connector design directly affects the mechanical behavior of FDPs. However, the effect of the volume and geometry of the pontic region, the main structure transmitting force to the connectors, on fracture strength has not been sufficiently investigated. While connector dimensions determine the cross-sectional area at the stress concentration point, pontic volume governs the overall stiffness, moment of inertia, and load distribution of the entire framework. These two parameters therefore represent conceptually distinct design variables, and modifying pontic volume independently of connector geometry constitutes a separate biomechanical intervention whose mechanical consequences have not been systematically evaluated in metal-ceramic fixed prostheses. A limited number of studies on pontic design have compared three pontic designs in implant-supported all-ceramic three-unit prostheses but have not reported statistically significant differences among them [13]. Similarly, Othman et al. [14] investigated whether different pontic geometries alone significantly affected fracture strength in implant-supported monolithic zirconia restorations. In the current literature, studies examining the specific effects of pontic volume and shape on fracture strength in metal-supported porcelain FDPs are limited. This information gap makes it difficult for clinicians to determine the optimal prosthesis design.

The aim of this study was to evaluate the effect of pontic volume on fracture strength in three-unit FDPs using a two-stage approach. In the first stage, metal substructures (cobalt-chromium, Co-Cr) with three different pontic volume configurations were tested to determine the pure effect of pontic volume change on frame mechanics. In the second stage, the impact of feldspathic porcelain veneer coating on the volume-fracture strength relationship of the brittle veneer layer was investigated. This two-stage design aims to reveal the difference between the ductile behavior of the metal substructure and the brittle fracture mechanics of the porcelain-covered restoration in the context of pontic volume. The findings are intended to provide mechanistic in vitro evidence regarding the biomechanical consequences of pontic volume modification, which may serve as a basis for future clinical and fatigue-based investigations. The null hypothesis of this study is that changes in pontic volume do not affect the fracture strength of FDPs with metal substructures and porcelain coverings.

## Materials and methods

### Preparation of die models, experimental groups

In the study model, 60 stainless steel die models were designed for three-unit FDPs consisting of second premolar and second molar abutment teeth and a first molar pontic tooth in the posterior mandibular region. All tooth anatomy was modeled using computer-aided design (CAD) software (exocad, exocad GmbH, Darmstadt, Germany) based on standard tooth anatomy references. The abutments were prepared with a 1.2 mm axial wall reduction, a 1.5 mm occlusal reduction, and a chamfer finish line. A ridge lap pontic form was used in the gingival region. This form was selected because it represents one of the most frequently used posterior pontic morphologies and provides a standardized, reproducible gingival contour; keeping the pontic form constant ensured that pontic volume remained the only independent variable across all groups [3]. The connector dimensions were standardized to $4 \times 4$ mm for all models. This standardization was deliberately maintained to isolate the mechanical effect of pontic volume from that of connector geometry, recognizing that these represent distinct design variables. To evaluate the effect of pontic volume on fracture resistance, three pontic volume

**Table 1** Pontic dimensions for each volume configuration

| Configuration | O-G (mm) | B-L (mm) | M-D (mm) | *n* (metal) | *n* (porcelain) |
|---|---|---|---|---|---|
| Small | 8.0 | 10.0 | 11.0 | 10 | 10 |
| Medium | 9.2 | 11.5 | 12.65 | 10 | 10 |
| Large | 10.4 | 13.0 | 14.3 | 10 | 10 |

configurations were designed. Small (S), Medium (M), and Large (L). The abutment tooth design was kept constant across all configurations; only the pontic volume was systematically varied. The pontic dimensions for each configuration are presented in Table 1. For each volume configuration, 10 metal-only cobalt-chromium (Co-Cr) alloy frameworks (Sm, Mm, Lm) and 10 feldspathic porcelain-veneered specimens (1.5 mm veneer thickness; VITA VM 13, VITA Zahnfabrik, Bad Säckingen, Germany) (Sp, Mp, Lp) were fabricated, yielding a total of 60 specimens ($n = 10$/group). The sample size of 10 specimens per group is consistent with established practice in comparable in vitro FDP fracture studies [8, 10, 13]. A sensitivity analysis (one-way ANOVA; three groups; $n = 10$ per group; $\alpha = 0.05$; power = 0.80) indicated that this design was sufficient to detect a large effect size (Cohen's $f \approx 0.62$). The effect sizes observed in the present study were substantially larger ($\eta^2 \approx 0.62$ for the metal and 0.57 for the porcelain groups), confirming adequate statistical power to detect the reported differences. Metal-only specimens were tested first to isolate the effect of pontic volume on framework mechanics; porcelain-veneered specimens were subsequently tested to examine the change in fracture behavior after porcelain veneering.

### Specimen fabrication

All Co-Cr alloy frameworks were fabricated using the Concept Laser Mlab laser melting system (Concept Laser Mlab, GE Additive, Lichtenfels, Germany). Digital designs were exported as STL files using exocad. After sintering, a stress relief heat treatment was applied at 1200 °C for 60 min. Surfaces were sandblasted with 50 µm aluminum oxide particles at 2.5 bar pressure and ultrasonically cleaned in distilled water.

### Porcelain veneer application

The porcelain veneer thickness was set at 1.5 mm, the standard value recommended in the literature for posterior metal-ceramic restorations [3, 15]. Following surface preparation, an oxidation process was applied at the manufacturer's recommended temperature and time to form a metal oxide layer [16]. Feldspathic porcelain (VITA VM 13, VITA Zahnfabrik, Bad Säckingen, Germany) was applied according to the manufacturer's protocol [17, 18]. Opaque porcelain was applied in a thin layer and fired under vacuum. Dentin porcelain was applied in multiple layers, and each layer was fired at the recommended temperature parameters. Surface characterization and glazing were completed according to standard procedure. All firing cycles were performed in a dental porcelain furnace (Programat P310, Ivoclar Vivadent AG, Schaan, Liechtenstein). A silicone indexing system derived from the CAD model was used to ensure uniform veneer thickness [19]. After each application, the target porcelain thickness of 1.5 mm was verified by digital caliper measurements taken at three points on the buccal, lingual, and occlusal surfaces. The acceptable tolerance was defined as ± 0.1 mm.

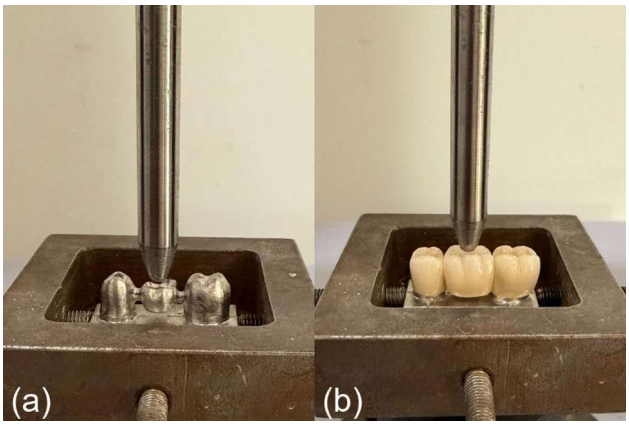



**Fig. 1** Experimental setup for fracture testing. **a** Metal specimen only, **b** Porcelain-veneered specimen mounted on a rigid support base

### Compression test of the specimens

Metal-ceramic FDPs were placed in a universal testing machine (AGS-X, Shimadzu Corp., Kyoto, Japan) for fracture resistance testing. Experiments were conducted and data recorded using the machine's TRAPEZIUM-X® software. Time (s), force (N), and displacement (mm) data were recorded simultaneously for each specimen during the test; these raw data were used in the analysis. During experimental apparatus setup, the specimens were positioned on a rigid sub-support and aligned so that the loading axis was at the center of the specimen. Compressive load was applied with a 5 mm diameter stainless steel tip from the central fossa of the pontic along the long axis of the restoration at a cross-head velocity of 0.5 mm/min until fracture occurred (Fig. 1) [20]. In this study, fracture behavior was evaluated separately for porcelain and metal specimen groups.

### Finite element analysis

Three-dimensional FEA was performed to evaluate the stress distributions in the metal frameworks. CAD data obtained from three metal framework models (Sm, Mm, Lm) were imported into FEA software (ANSYS Workbench 2023 R1, ANSYS Inc., Canonsburg, PA, USA). The Co-Cr alloy was modeled as linear elastic, homogeneous,

and isotropic (E = 218 GPa, ν = 0.33) [16, 21]. Although this assumption simplifies the actual material behavior, it is a standard approach for comparative stress analysis within the elastic region and is consistent with similar FEA studies in the literature [4, 6, 7]. The porcelain veneer layer was not included in the FEA model; the analysis was limited to the metal framework to isolate the effect of pontic volume on framework-level stress distribution and to maintain compatibility with the linear elastic material assumption.

The mesh structure consisted of tetrahedral elements with an average element size of 0.30–0.35 mm. Local mesh refinement was applied in the occlusal contact and connector regions. A mesh convergence study confirmed that the von Mises stress values became independent of the number of elements at approximately 185,000 elements and 265,000 nodes. The base surfaces of all models were fully fixed in all directions. A vertical load of 500 N was applied as a distributed load on the occlusal surface of the metal framework. Although this load level is within the range of physiological masticatory forces reported in the posterior region (300–800 N), the FEA results are intended for comparative purposes only and do not represent absolute failure predictions. This load value was selected to ensure that the material remains in the linear-elastic region and to represent physiological chewing forces. Beyond this mesh-convergence verification, the model was further assessed against the experimental data. Although this linear-elastic analysis at a single subfracture load (500 N) was not intended to predict the absolute fracture load, its validity was supported by two findings: the location of the maximum von Mises stress coincided with the fracture-initiation region observed in all groups, and the stress ordering between configurations was inversely consistent with the measured fracture-load ordering.

**Table 2** Fracture load values (*N*) of metal and porcelain groups

| Groups | *n* | Mean ± SD (*N*) | F | *P*(ANOVA) |
|---|---|---|---|---|
| Sm | 10 | 5284.1 ± 228.85[a] | 22.135 | < 0.001* |
| Mm | 10 | 5659.8 ± 246.70[b] | | |
| Lm | 10 | 6093.5 ± 330.34[c] | | |
| Sp | 10 | 1506.0 ± 183.41[a] | 17.784 | < 0.001* |
| Mp | 10 | 1724.4 ± 144.38[b] | | |
| Lp | 10 | 1935.8 ± 153.06[c] | | |

Different superscript letters (a, b, c) indicate statistically significant differences (Tukey HSD, $P < .05$)

*Sm* Small metal, *Mm* Medium metal, *Lm* Large metal, *Sp* Small porcelain, *Mp* Medium porcelain, *Lp* Large porcelain

*$P$<.05 is statistically significant (One-way ANOVA, Tukey HSD post-hoc test). Metal Sm–Mm $P$=.013, Sm–Lm $P$<.001, Mm–Lm $P$=.004; Porcelain Sp–Mp $P$=.014, Sp–Lp $P$<.001, Mp–Lp $P$=.018

### Statistical analysis

Statistical analysis of the obtained data was performed using the Python programming language (version 3.11) and the SciPy statistical library (version 1.11). Descriptive statistics (mean and standard deviation) were calculated for all groups. The normality of the data distribution was assessed using the Shapiro-Wilk test, and the homogeneity of variances was assessed using the Levene test. After confirming that the assumptions of normal distribution and homogeneity of variances were met, one-way analysis of variance (ANOVA) was used to compare the fracture load values within the metal and porcelain groups. If a statistically significant difference was detected as a result of the ANOVA, the Tukey HSD (Honestly Significant Difference) post-hoc test was applied for pairwise comparisons between groups. The statistical significance level was accepted as $P$<.05.

## Results

The average fracture loads in the metal group as a result of the compression test were measured as Small (Sm): 5284.1 ± 228.85 N, Medium (Mm): 5659.8 ± 246.70 N, and Large (Lm): 6093.5 ± 330.34 N. In the porcelain group, the values obtained were Small (Sp): 1506.0 ± 183.41 N, Medium (Mp): 1724.4 ± 144.38 N, and Large (Lp): 1935.8 ± 153.06 N. One-way ANOVA analysis revealed statistically significant differences both between the metal groups ($F$ = 22.135, $P$<.001) and between the porcelain groups ($F$ = 17.784, $P$<.001). The post-hoc Tukey HSD test showed statistically significant differences in all pairwise comparisons (Sm vs. Mm: $P$=.013, Sm vs. Lm: $P$<.001, Mm vs. Lm: $P$=.004; Sp vs. Mp: $P$=.014, Sp vs. Lp: $P$<.001, Mp vs. Lp: $P$=.018) (Table 2).

Figure 2 shows the force-dependent deformations after compression testing on three-unit crowns with metal substructures, produced in different volumes. In the graph, the smallest-volume model (Small model-Sm) initially increases linearly with a low slope. In this model, the amount of deformation increases as the compressive force increases, reaching a maximum force between 2.5 and 3 mm before fracture occurs, followed by a rapid decrease in force. However, the maximum force it can carry is lower than that of other models. Early fracture onset and rapid crack propagation were observed in the connector region (Fig. 3a-b). The medium volume model (Mm) has a higher slope than the Sm model. The force value and deformation amount reach their highest value at approximately 2.5 mm. A sudden force drop occurred after this point (Fig. 3c-d). The large-volume model (Lm) reached the highest fracture load compared to the other models. The deformation was quite low with increasing force. Pre-fracture plastic deformation traces were observed in Fig. 3. When the three groups are evaluated together, fracture load increased as the pontic

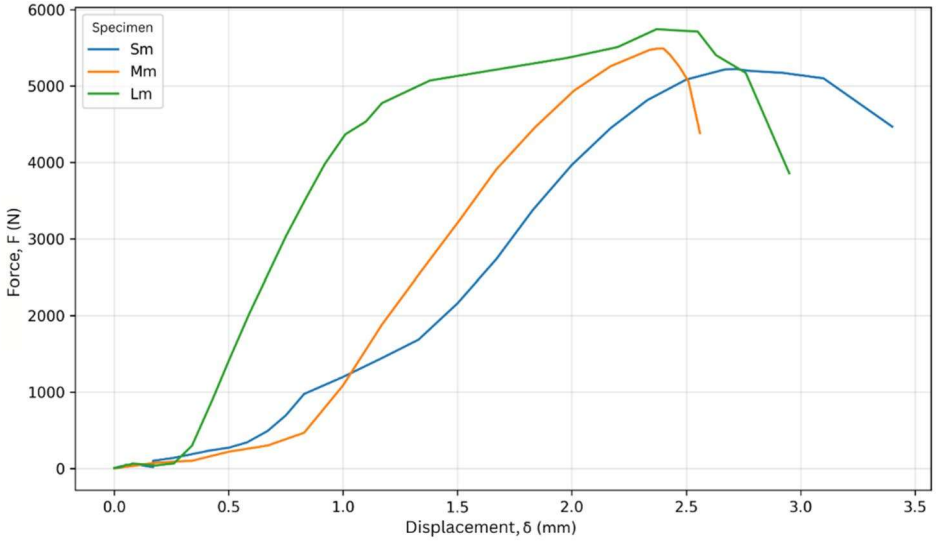



**Fig. 2** Force-displacement curves of the metal group

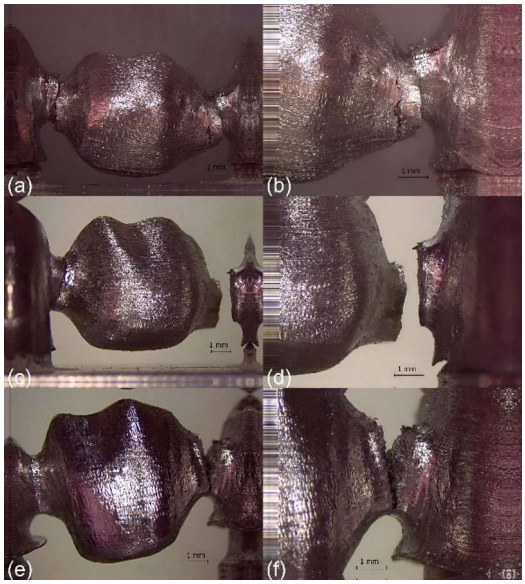



**Fig. 3** Stereomicroscope fracture images of metal samples after compression testing. **a**-**b**) Small model (Sm), **c**-**d**) Medium model (Mm), **e**-**f**) Large model (Lm)

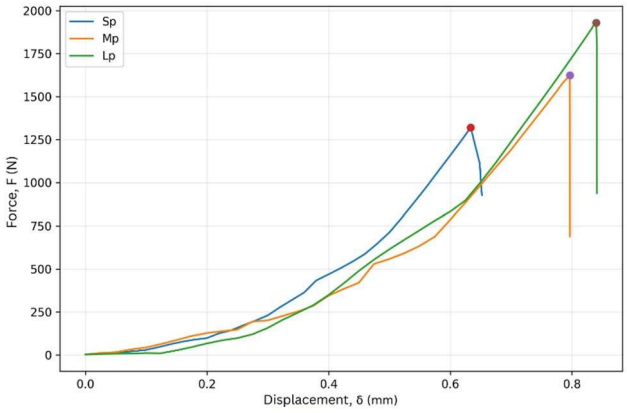



**Fig. 4** Force-displacement curves of the porcelain group

volume increased. Sudden force drops after fracture were observed in the large-volume model. Failure in all metal groups occurred predominantly in the connector-pontic junction region.

When the fracture response of the porcelain specimens was evaluated via F–δ curves, it was observed that the curves generally transitioned to a lower slope region initially followed by a main load-carrying region where the load-carrying capacity increased. As the size increased, the force carried in the same displacement ranges increased, and higher capacity was maintained until the peak load was reached. Force decreased markedly after the peak load. The force-displacement curves of the specimens are presented in Fig. 4. The small porcelain-veneered model (Small Porcelain model – Sp) allowed for a small amount of deformation with increasing force. Once the deformation reached approximately 0.6 mm, the maximum load was achieved. Images in Figs. 5a-b, taken after fracture, show that a brittle fracture occurred in the porcelain material, causing the porcelain coating to separate from the bonding area.

The medium-volume porcelain-veneered model (Mp) carried a higher force than the Sp model, and a sudden drop was recorded at the fracture point. Figures 5c-d show that the cracking started at the connector points and progressed as a wide-diameter crack. In contrast, the large-volume porcelain-veneered model (Lp) yielded the highest force value. However, the sharp drop after reaching the maximum force shows that the brittle fracture behavior of the porcelain layer again governed failure (Figs. 5e-f). The cracks in the porcelain coating are

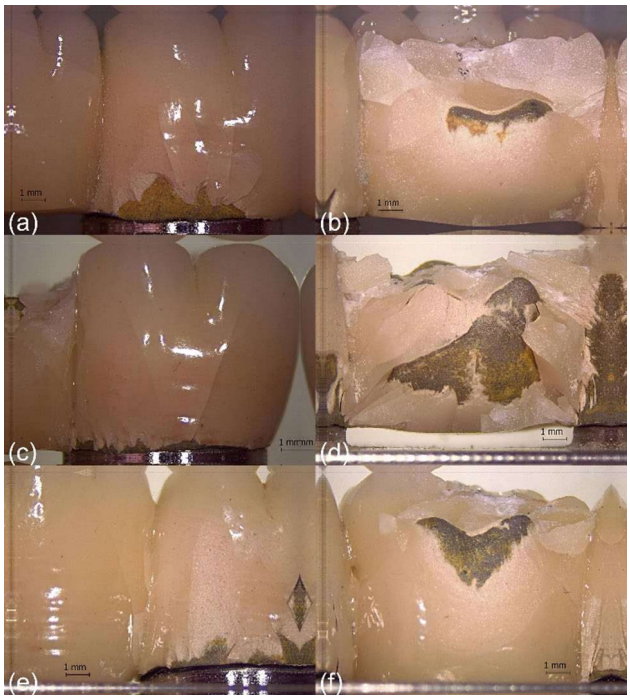



**Fig. 5** Stereomicroscope fracture images of porcelain specimens after compression testing. **a**-**b**) Small porcelain model (Sp), **c**-**d**) Medium porcelain model (Mp), **e**-**f**) Large porcelain model (Lp)

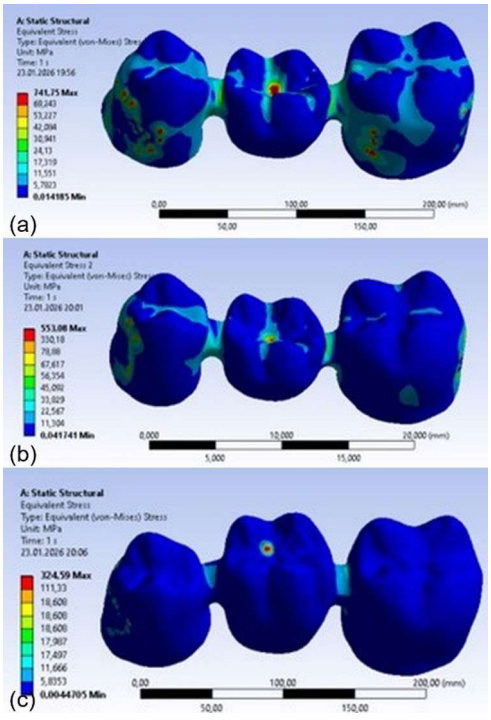



**Fig. 6** Finite element analysis of von Mises stress distributions. **a**-**c**) Metal substructure models (Sm, Mm, Lm)

smaller, and the visibility of the metal substructure is reduced. In all porcelain groups, fracture occurred in the connector-pontic transition region. Fracture occurred primarily as cracking of the porcelain layer and separation from the metal-porcelain interface, without significant plastic deformation in the metal substructure.

After determining the force-displacement relationship from the in vitro compression test, FEA was conducted to examine in detail the stresses in the prostheses, to corroborate the experimental findings, and to verify the numerical stability of the model (Fig. 6). The changes in metal-based systems are shown in Figs. 6a-c. In the Sm model, the von Mises stress reached approximately 740 MPa, which is close to the yield strength of the Co-Cr alloy. This was observed to occur primarily at the pontic connector necks. It is consistent with the crack locations shown in the images in Fig. 3 after the in vitro compression test. In the Mm model, the maximum stress is around 550 MPa, and it was observed that the stress was spread over a wider area compared to the Sm model. In the Lm model, the maximum stress is approximately 325 MPa, and the stress distribution was homogeneous on the surface and remained well below the yield strength of the Co-Cr alloy. The maximum stress is concentrated at the pontic-abutment connector neck, and a decrease in maximum stress is observed as the pontic volume increases.

## Discussion

FEA has been used to evaluate multiple factors affecting the fracture strength of FDPs in prosthetic dentistry. These evaluations have examined the fracture strength of three-unit FDPs by modifying design parameters such as connector design and size, connector height, and veneer-frame thickness ratio [4–7]. However, no study has examined the independent effect of pontic volume, with connector dimensions held constant, on the fracture behavior of metal-ceramic FDPs using both in vitro testing and FEA validation. While the general principle that larger structural cross-sections reduce stress concentration is well established in mechanics, the clinical question of whether pontic volume constitutes an actionable and isolable design parameter in metal-ceramic FDPs required direct experimental verification. In the present study, experimental and numerical results corroborated one another: FEA results showed that stress concentrations decreased and stress distribution became more homogeneous with increasing pontic volume, and in vitro fracture tests revealed parallel increases in fracture load. Despite the development of new materials, metal-porcelain restorations remain widely used in clinical practice [22].

In their FEA study, Alberto et al. [6] investigated the fracture resistance of implant-supported restorations by

varying the connector height. The same study reported that in zirconia-supported, implant-supported 3-unit FDPs, models with larger distal connectors (4 and 5 mm) exhibited lower stresses and a more even distribution than the model with the smallest distal connector. In their FEA study investigating various connector sizes using 3-unit all-ceramic and metal-supported porcelain as the control group, Bataineh et al. [7] concluded that the size of different posterior all-ceramic three-unit FDP connectors significantly affected the long-term survival of prostheses. Their results showed that fatigue resistance increased with connector size, ranging from 670 N for the largest connector (4 × 3 mm) to 273 N for the smallest connector (3.5 × 2.5 mm) in zirconia. In the current study, FEA revealed a significant decrease in maximum von Mises stress as the pontic volume increased. Furthermore, the analyses showed that changes in pontic design affected not only the maximum stress values but also the stress distribution pattern within the structure. It should be noted that the FEA model in the present study was limited to the metal framework and did not incorporate the porcelain veneer layer. This simplification was intentional: including the viscoelastic behavior and residual thermal stresses of feldspathic porcelain in a linear elastic model would introduce assumptions that cannot be reliably validated. Consequently, the FEA results should be interpreted as framework-level comparative stress indicators rather than absolute stress predictions for the complete metal-ceramic system. Future studies incorporating multi-layer FEA models with thermomechanical boundary conditions would provide a more complete characterization of interfacial stress behavior. Designs that provide a homogeneous stress distribution prevent localized stress concentrations and increase the overall strength of the structure. The fracture behavior differed markedly between the metal and porcelain groups. In the metal group, fracture mode transitioned from more ductile (Sm) to relatively less ductile (Lm) as pontic volume and framework rigidity increased. This pattern is consistent with the higher moment of inertia of larger cross-sections. In the porcelain-veneered group, brittle fracture dominated across all volume configurations, with crack initiation consistently observed at the connector-pontic junction. This reflects the inability of the feldspathic porcelain to accommodate the elastic deformation of the underlying Co-Cr framework, resulting in interfacial stress accumulation and delamination regardless of pontic volume.

In an in vitro study in which direct fracture testing was performed without FEA, Larsson et al. [10] concluded that the fracture resistance of the zirconium scaffold, in which four-unit FDPs with connector dimensions of 2.0, 2.5, 3.0, 3.5, and 4.0 mm were tested, increased significantly with increasing connector diameter. Although not in metallic substructures, many studies on the fracture resistance of FDPs have investigated and reported the effects of the connector area and connector design in the literature [8, 9, 23]. Oh and Anusavice [8] investigated the impact of connector design on fracture resistance in all-ceramic FDPs and reported that increasing connector dimensions significantly improved fracture resistance. In another study by the same researchers, [9] the effect of connector design on the fracture probability of porcelain FDPs was evaluated, and it was concluded that wider connector cross-sections significantly reduced the risk of fracture. Studart et al. [23] investigated the fatigue behavior of zirconia under cyclic loading in an aqueous environment, emphasizing that connector dimensions directly affect fatigue life in the design of dental bridges and that determining the optimal connector cross-section is critical for clinical success. A common finding across these studies is that increasing connector dimensions improves both static fracture strength and fatigue resistance. The wide range of reported fracture loads in the literature is likely due to factors in the test configuration that significantly affect the mechanical response. Parameters such as indenter geometry, interlayer use, support conditions, and loading configuration are thought to alter the contact pressure directly and thus the stress distribution.

Studies investigating the effect of pontic design on fracture strength have reported varying results. Inan et al. [13] compared the fracture strengths of implant-supported all-ceramic 3-unit FDPs using three different pontic designs in their in vitro study. Although the different designs had different fracture resistances, they reported no statistically significant difference between these fracture values. Othman et al. [14] investigated the effect of different pontic designs (ovate, modified ridge lap, sanitary) on the fracture strength of implant-supported monolithic zirconia FDPs and reported that pontic design did not significantly affect fracture strength. In the study, all pontic designs showed fracture values between 1424 and 1430 N, and it was stated that these values were significantly higher than regular chewing forces (285–462 N). It should be emphasized that the fracture loads recorded in all groups of the present study, including the smallest porcelain-veneered configuration (≈ 1506 N), also greatly exceeded this range. The clinical relevance of increasing pontic volume therefore lies not in preventing failure under routine chewing which all designs withstand with a wide margin but in the larger safety reserve it provides against occasional supra-functional loads, such as those generated during parafunction or bruxism [24, 25]. This distinction is clinically relevant, since bruxism markedly increases the mechanical failure of fixed restorations: in a matched cohort, tooth-supported metal-ceramic FDPs failed more frequently

in bruxers than in non-bruxers (32.3% vs. 25.8%), with major porcelain chipping occurring exclusively in bruxers [24], and the risk of metal-ceramic defects has been reported to be approximately 2.5 times higher in bruxers [25]. Since static fracture strength is generally considered an indicator of fatigue resistance, the increase in load-carrying capacity along with an increase in pontic volume can positively affect long-term performance under cyclic intraoral loading. This assessment is supported by current experimental data showing that volume increase affects not only the maximum fracture load but also the stiffness and post-peak fracture behavior of the specimens. These findings demonstrate that pontic volume plays a role in the load-transmission behavior of the restoration. It was shown that pontic designs alone do not affect fracture strength, even without a metal substructure [13, 14]. Unlike these pontic-shape comparisons, the present study isolated pontic volume and showed that increasing it significantly improved fracture resistance, particularly in porcelain-veneered restorations. Whether this translates into a clinically viable strategy particularly in cases with recurrent restoration failure where aesthetic considerations are secondary requires validation through fatigue-based and prospective clinical studies before definitive recommendations can be made. In the literature on fracture tests, it is generally accepted that the static load-carrying capacity of restorative systems is governed by stress concentrations arising from geometry rather than by material properties. In particular, in FDPs, attachment areas are considered critical regions because of their small cross-sectional area and sharp transitions, which lead to stress concentration [7, 26]. In this context, the peak load and subsequent behavior observed in the experiments were consistent with the stress distribution and the areas of cross-sectional change in the region where the load was transmitted. Nevertheless, the clinical extrapolation of static fracture data should be approached with caution, as monotonic loading conditions do not replicate the cyclic, thermally variable, and moisture-rich environment of the oral cavity.

The main limitation of this study is that fracture tests were performed under monotonic compressive loading in a dry environment and without thermal cycling, whereas clinical failures are shaped by time-dependent mechanisms such as fatigue, thermal cycling, moisture effects, and interfacial degradation. The periodontal ligament was excluded from the FEA boundary conditions; although this is consistent with the rigid support configuration used in the in vitro test, it limits the physiological relevance of the stress distribution results. The porcelain veneer and cement layer were not included in the model; the absence of the cement layer assumes a rigid bond at the restoration–abutment interface and may therefore overestimate framework stiffness. While keeping the connector dimensions constant across all models isolates the effect of pontic volume, this approach also has a limitation: the connector geometry will change as pontic volume varies in clinical practice. Finally, pontic volume was increased by scaling the occlusogingival, buccolingual, and mesiodistal dimensions simultaneously (Table 1), so the effect reflects the combined geometric change rather than any single dimension; isolating individual contributions would require varying one dimension at a time. The connector cross-section, however, was held constant ($4 \times 4$ mm), so the effect is independent of connector geometry.

## Conclusion

Increasing the pontic volume improves fracture resistance in both metal-based and porcelain-veneered restorations. FEA results support this finding, with a significant decrease in maximum von Mises stress values at the connector-pontic junction as the pontic volume increases. These results suggest a potential biomechanical advantage for larger pontic volumes; however, clinical usefulness remains unproven and should be evaluated in fatigue-based and prospective studies.

### Abbreviations

| | |
|---|---|
| ANOVA | Analysis of Variance |
| CAD | Computer-Aided Design |
| Co-Cr | Cobalt-Chromium (alloy) |
| FDP / FDPs | Fixed Dental Prosthesis / Prostheses |
| FEA | Finite Element Analysis |
| HSD | Honestly Significant Difference (Tukey post-hoc test) |
| L / Lm / Lp | Large / Large metal / Large porcelain-veneered specimen |
| M / Mm / Mp | Medium / Medium metal / Medium porcelain-veneered specimen |
| S / Sm / Sp | Small / Small metal / Small porcelain-veneered specimen |

## Supplementary Information

The online version contains supplementary material available at https://doi.org/10.1186/s12903-026-09111-x.

Supplementary Material 1.

Supplementary Material 2.

### Acknowledgements

Not applicable.

### Authors' contributions

Buse Cebi Gul: Conceptualization, Methodology, Validation, Investigation, Resources, Data curation, Writing - original draft, Writing - review & editing, Visualization, Supervision. Erkan Bahce: Conceptualization, Methodology, Data Curation, Validation, Writing-review & editing, supervision. Adem Atmaca: Methodology, Data Curation, Validation. Furkan Kuzudisli: Methodology, Data Curation, Resources. Fatih Demirci: Methodology, Writing-review & editing, supervision.

### Funding

No funding.

### Data availability

The data that support the findings of this study are available from the corresponding author upon reasonable request.

## Declarations

**Ethics approval and consent to participate**
Not applicable. This study did not involve human participants, human data, human tissue, or animal subjects. The research was conducted entirely using in vitro laboratory specimens and finite element analysis; therefore, ethical approval and informed consent were not required.

**Consent for publication**
Not applicable.

**Competing interests**
The authors declare no competing interests.

Received: 14 April 2026 / Accepted: 24 June 2026
Published online: 10 July 2026

**References**

1. Shillingburg HT, Hobo S, Whitsett LD, Jacobi R, Brackett SE. Fundamentals of fixed prosthodontics., IL, USA: Quintessence Publishing Company Chicago; 1997.
2. Shen C, Rawls HR, Esquivel-Upshaw JF. Phillips' Science of Dental Materials E-Book: Phillips' Science of Dental Materials. E-Book: Elsevier Health Sciences; 2021.
3. Rosenstiel SF, Land M, Fujimoto J. Contemporary Fixed Prosthodontics-E-Book. Sr. Louis. Missouri, USA: Elsevier Health Sciences; 2015.
4. Alberto LHJ, Kalluri L, Esquivel-Upshaw JF, Duan Y. Three-dimensional finite element analysis of different connector designs for all-ceramic implant-supported fixed dental prostheses. Ceramics. 2022;5(1):34–43.
5. Kalluri L, Seale B, Satpathy M, Esquivel-Upshaw JF, Duan Y. Three-dimensional finite element analysis of the veneer—framework thickness in an all-ceramic implant supported fixed partial denture. Ceramics. 2021;4(2):199–207.
6. Alberto LHJ, Kalluri L, Esquivel-Upshaw JF, Duan Y. Finite element analysis of an implant-supported FDP with different connector heights. Symmetry. 2022;14(11):2334.
7. Bataineh K, Al Janaideh M, Abu-Naba'a LA. Fatigue resistance of 3-unit CAD-CAM ceramic fixed partial dentures: an FEA study. J Prosthodont. 2022;31(9):806–14.
8. Oh W-s, Anusavice KJ. Effect of connector design on the fracture resistance of all-ceramic fixed partial dentures. J Prosthet Dent. 2002;87(5):536–42.
9. Oh Ws, Götzen N, Anusavice KJ. Influence of connector design on fracture probability of ceramic fixed-partial dentures. J Dent Res. 2002;81(9):623–7.
10. Larsson C, Holm L, Lövgren N, Kokubo Y, Vult von Steyern P. Fracture strength of four-unit Y-TZP FPD cores designed with varying connector diameter. An in-vitro study. J Oral Rehabil. 2007;34(9):702–9.
11. Ogino Y, Nomoto S, Sato T. Effect of connector design on fracture resistance in zirconia-based fixed partial dentures for upper anterior region. Bull Tokyo Dent Coll. 2016;57(2):65–74.
12. Tatarciuc M, Maftei GA, Vitalariu A, Luchian I, Martu I, Diaconu-Popa DJAS. Inlay-retained dental bridges—a finite element analysis. Appl Sci. 2021;11(9):3770.
13. Inan O, Secilmis A, Eraslan O. Effect of pontic framework design on the fracture resistance of implant-supported all-ceramic fixed partial dentures. J Appl Oral Sci. 2009;17(5):533–8.
14. Othman MS, Abu-Eittah MR. The influence of different pontic designs on fracture resistance of implant-supported fixed partial dentures anchored in polyurethane simulating bone-blocks of two different densities: an in vitro study. J Contemp Dent Pract. 2024;25(7):684–90.
15. Goodacre CJ, Campagni WV, Aquilino SA. Tooth preparations for complete crowns: an art form based on scientific principles. J Prosthet Dent. 2001;85(4):363–76.
16. Wataha JC. Alloys for prosthodontic restorations. J Prosthet Dent. 2002;87(4):351–63.
17. Anusavice KJ, Kakar K, Ferree N. Which mechanical and physical testing methods are relevant for predicting the clinical performance of ceramic-based dental prostheses? Clin Oral Implants Res. 2007;18(Suppl 3):218–31.
18. Benetti P, Kelly JR, Sanchez M, Della Bona A. Influence of thermal gradients on stress state of veneered restorations. Dent Mater. 2014;30(5):554–63.
19. Zarauz C, Valverde A, Martinez-Rus F, Hassan B, Pradies G. Clinical evaluation comparing the fit of all-ceramic crowns obtained from silicone and digital intraoral impressions. Clin Oral Investig. 2016;20(4):799–806.
20. Demirci F, Bahce E, Baran MC. Mechanical analysis of three-unit metal-free fixed dental prostheses produced in different materials with CAD/CAM technology. Clin Oral Investig. 2022;26(9):5969–78.
21. Kelly JR, Benetti P. Ceramic materials in dentistry: historical evolution and current practice. Aust Dent J. 2011;56(Suppl 1):84–96.
22. Pjetursson BE, Sailer I, Makarov NA, Zwahlen M, Thoma DS. All-ceramic or metal-ceramic tooth-supported fixed dental prostheses (FDPs)? A systematic review of the survival and complication rates. Part II: Multiple-unit FDPs. Dent Mater. 2015;31(6):624–39.
23. Studart AR, Filser F, Kocher P, Gauckler LJJD. Fatigue of zirconia under cyclic loading in water and its implications for the design of dental bridges. Dent Mater. 2007;23(1):106–14.
24. Hawthan M, Chrcanovic BR, Larsson C. Retrospective study comparing clinical outcomes of fixed dental prostheses in matched groups of bruxer and nonbruxer patients. Int J Dent. 2022;2022:6818170.
25. Reitemeier B, Hänsel K, Kastner C, Weber A, Walter MH. A prospective 10-year study of metal ceramic single crowns and fixed dental prosthesis retainers in private practice settings. J Prosthet Dent. 2013;109(3):149–55.
26. De Jager N, Pallav P, Feilzer AJ. The influence of design parameters on the FEA-determined stress distribution in CAD-CAM produced all-ceramic dental crowns. Dent Mater. 2005;21(3):242–51.

## Publisher's note

Springer Nature remains neutral with regard to jurisdictional claims in published maps and institutional affiliations.